

Genetic Risk for Alzheimer Disease Is Distinct from Genetic Risk for Amyloid Deposition

Ganna Leonenko *, Maryam Shoai,²* Eftychia Bellou,¹ Rebecca Sims,¹ Julie Williams,^{1,3} John Hardy,^{2,4} and Valentina Escott-Price,^{1,3}
the Alzheimer's Disease Neuroimaging Initiative

Objective: Alzheimer disease (AD) is the most common form of dementia and is responsible for a huge and growing health care burden in the developed and developing world. The polygenic risk score (PRS) approach has shown 75 to 84% prediction accuracy of identifying individuals with AD risk.

Methods: In this study, we tested the prediction accuracy of AD, mild cognitive impairment (MCI), and amyloid deposition risks with PRS, including and excluding APOE genotypes in a large publicly available dataset with extensive phenotypic data, the Alzheimer's Disease Neuroimaging Initiative cohort. Among MCI individuals with amyloid-positive status, we examined PRS prediction accuracy in those who converted to AD. In addition, we divided polygenic risk score by biological pathways and tested them independently for distinguishing between AD, MCI, and amyloid deposition.

Results: We found that AD and MCI are predicted by both APOE genotype and PRS (area under the curve [AUC] = 0.82% and 68%, respectively). Amyloid deposition is predicted by APOE only (AUC = 79%). Further progression to AD of individuals with MCI and amyloid-positive status is predicted by PRS over and above APOE (AUC = 67%). In pathway-specific PRS analyses, the protein–lipid complex has the strongest association with AD and amyloid deposition even when genes in the APOE region were removed ($p = 0.0055$ and $p = 0.0079$, respectively).

Interpretation: The results showed different pattern of APOE contribution in PRS risk predictions of AD/MCI and amyloid deposition. Our study suggests that APOE mostly contributes to amyloid accumulation and the PRS affects risk of further conversion to AD.

ANN NEUROL 2019;86:427–435

Alzheimer disease (AD) is the most common form of dementia in elderly people and is a major health problem worldwide.¹ The clinical diagnosis is typically characterized by progressive loss of memory and cognitive function. In the past decade, numerous relevant susceptibility loci, genes, and pathways have been identified^{2–6} that have improved the understanding of this complex disease. However, the risk for developing AD involves multiple

genetic and environmental components, with the *APOE* genotype⁷ having the strongest genetic effect.²

Amyloid-beta (A β) plays a key role in the pathogenesis of AD, but little is known about the process of its formation in the brain. Identification of the earliest pathological signature of AD requires longitudinal measurements of A β deposition in the brain by positron emission tomography (PET) or by measurements of A β reduction in

View this article online at wileyonlinelibrary.com. DOI: 10.1002/ana.25530

Received Mar 12, 2019, and in revised form Jun 11, 2019. Accepted for publication Jun 12, 2019.

Address correspondence to Dr Escott-Price, Dementia Research Institute, Hadyn Ellis Building, Cardiff University, Maindy Road, Cardiff, CF24 4HQ, United Kingdom. E-mail: escottpricev@cardiff.ac.uk

*G.L. and M.S. are joint first authors.

Data used in the preparation of this article were obtained from the Alzheimer's Disease Neuroimaging Initiative (ADNI) database (<http://adni.loni.usc.edu>). As such, the investigators within the ADNI contributed to the design and implementation of ADNI and/or provided data but did not participate in analysis or the writing of this report. A complete listing of ADNI investigators is available at http://adni.loni.usc.edu/wp-content/uploads/how_to_apply/ADNI_Authorship_List.pdf.

From the ¹Medical Research Council Centre for Neuropsychiatric Genetics and Genomics, Cardiff University, Cardiff; ²Reta Lilla Research Laboratories, Department of Neurodegeneration and UK Dementia Research Institute, University College London Institute of Neurology, London; ³UK Dementia Research Institute at Cardiff University, Cardiff; and ⁴UK Dementia Research Institute at University College London, London, United Kingdom

cerebrospinal fluid (CSF). Although A β is necessary for the pathologic diagnosis of AD, it is not sufficient in itself to cause cognitive dysfunction and clinical AD. It has been shown that amyloid deposition has low specificity for predicting development of AD.^{8,9}

The preclinical stage of AD starts with mild impairment in cognitive domains (MCI) and includes a syndrome featuring relatively isolated memory deficits.¹⁰

In 2011, the National Institute on Aging and Alzheimer's Association created separate sets of diagnostic guidelines for the symptomatic or "clinical" stages of AD,^{11,12} where AD represents the "disease" and "dementia" represents the clinical syndrome. Thus, a person may progress from MCI to dementia (due to AD), but both MCI and dementia cases may or may not be AD.

Studying individuals who develop MCI and then further progress to AD requires detailed longitudinal datasets. The Alzheimer's Disease Neuroimaging Initiative (ADNI) is a multicenter study designed to assess the utility of various biomarkers for detecting early changes associated with MCI and AD. It includes collection of neuroimaging data, clinical and cognitive assessments, and information on demographics and individual genetic profiles.

The polygenic risk score (PRS) approach aggregates the effects of multiple genetic markers identified through genome-wide association studies (GWASs)² and has shown great potential in identifying an individual's risk of developing AD.^{13,14} A few studies have recently used AD PRS to predict mild cognitive functions and clinical MCI¹⁵; however, only one has suggested that PRS could identify MCI in middle aged adults¹⁶ more effectively than the *APOE* locus alone. The PRS approach has also been applied to biological pathways related to AD but was not more predictive than *APOE* alone.¹⁷ The implementation of polygenic hazard score (PHS; closely related to PRS¹⁸) analysis in the ADNI data showed that PHS is associated with AD biomarkers (CSF and PET) in individuals without AD,¹⁹ and that higher PHS was associated with greater rates of cognitive and clinical decline, even after controlling for *APOE* status²⁰; however, its predictive value was not quantified.

In this study, we estimate the predictive accuracy of PRS differentiating (1) AD cases versus controls, (2) MCI cases versus controls, and (3) amyloid-positive versus amyloid-negative individuals. We also investigate whether (4) the AD PRS can predict individuals with MCI who will progress to AD and those who will remain with MCI, with positive amyloid deposition.

Recently, GWASs and exome/genome sequencing have implicated, with varying degrees of confidence, lipid metabolism, the innate immune system, and endosomal vesicle recycling in late onset AD pathogenesis.^{21,22}

Therefore, we also examined the pathway-specific PRS association using these recently identified pathways⁶ related to AD risk.

Materials and Methods

ADNI: Setting/Clinical Description

Data used in the preparation of this article were obtained from ADNI, a publicly available database (<https://adni.loni.usc.edu>). The primary goal of ADNI has been to test whether serial magnetic resonance imaging (MRI), PET, other biological markers, and clinical and neuropsychological assessment can be combined to measure the progression of MCI and early AD. The data were collected for about 900 individuals between ages 55 and 90 years. The initial 5-year study (ADNI1) followed participants for 2 to 3 years, with repeated imaging scans and psychometric measurements every 6 or 12 months. All ADNI participants provided written informed consent. The ADNI project was extended as the ADNI-GO and ADNI2, studies with a proportion of new and original ADNI1 participants.

Clinical diagnosis and genetic information were available for 770 individuals from the ADNI1, ADNI-GO, and ADNI2 studies. Longitudinal data contained information about clinical assessments from the first visit (baseline) to the latest available visit, with mean follow-up time of approximately 5 years. Details of the ADNI design, participant recruitment, clinical testing, and additional methods have been previously reported elsewhere.^{23,24}

Table 1 shows the classification of diagnosis and number of individuals whose diagnosis remained stable during the study. It also presents the diagnostic categories and the numbers of individuals within those diagnostic categories at the latest assessment, which were used for the analyses.

To assess amyloid deposition, the latest MRI PET scans from 663 participants were used in the analysis (AV45 ligand threshold of 1.11). In this study, we used the individuals' diagnosis at the latest point of assessment. We then tested whether AD PRSs were associated with AD, MCI, and amyloid status in 3 main analyses: (1) AD versus controls, (2) MCI versus controls, and (3) amyloid-positive versus amyloid-negative status (Table 2).

ADNI: Genotyping and Quality Control

A total of 770 samples from ADNI1/GO/2 set were whole-genome sequenced (WGS) and genotyped using the Illumina (San Diego, CA) Omni 2.5M BeadChip (42,732,452 variants). WGS calls were made using the Broad Institute best practices (BWA & GATK HaplotypeCaller).

Basic quality control checks were performed using standard procedure.²⁵ Single nucleotide polymorphisms (SNPs) were excluded where genotype missingness was >0.02, Hardy-Weinberg equilibrium *p* value was <1e-6, and SNP minor allele frequency was <0.01. This retained 7,808,548 SNPs for the analyses. Matching those SNPs with the latest publicly available GWAS AD summary statistics² reduced that number to 5,771,686.

TABLE 1. Clinical Classification of Diagnosis in ADNI Dataset

Diagnosis Description	Samples with Diagnosis at the First Time Point, n	Samples with Diagnosis at the Last Time Point, n	Samples Stable over Time, n	Usage for Analysis
Stable control to control	262	224	200	Controls
Stable MCI to MCI	459	289	267	MCI
Stable AD to AD	47	174	46	AD
Conversion control to MCI	0	20	0	Exclude
Conversion MCI to AD	1	50	0	MCI
Conversion MCI to control	1	8	0	Exclude
Conversion AD to MCI	0	5	0	MCI

Diagnosis description—classification of clinical diagnosis made for each participant and each time point. Second column shows number of participants with baseline diagnosis. Third column shows number of participants at the last point of diagnosis. Fourth column shows number of participants who did not change their diagnosis at the last assessment from baseline diagnosis. Last column shows clinical classification of individuals based on the last available diagnosis for our analyses.

AD = Alzheimer disease; ADNI = Alzheimer's Disease Neuroimaging Initiative; MCI = mild cognitive impairment.

Generating PRS

Generation of PRS requires 2 independent datasets: summary statistics of association with AD in a discovery sample; and a test sample, which is independent of the discovery sample and contains genotypes for each individual.²⁶ As the discovery sample, we used summary statistics from the powerful GWAS

(17,008 AD cases and 37,154 controls) of the International Genomics of Alzheimer's Project (IGAP Stage 1).² PRSs were generated using SNPs with AD association $p \leq 0.5$ in the IGAP dataset, as it has been reported as having the best prediction accuracy.¹³ The SNPs were then linkage disequilibrium (LD) pruned ($r^2 = 0.1$ and 1,000kb window), keeping the SNPs most associated with AD. The number of SNPs after the LD pruning was 162,957. We included *APOE* ε2 and ε4 allele genotypes directly into the PRS with effect sizes $B = -1.04$ and $B = 1.55$ for ε2 and ε4, respectively, calculated in the ADNI data, while excluding the *APOE* region (chromosome 19:44,400–19:46,500kb).¹³ Prior to all analyses, the PRSs were adjusted for the 8 principal components and then standardized.

A total of 441 ADNI participants were part of original IGAP summary statistics.² To overcome a potential bias in PRS analysis due to overlapping samples, we used a simulation approach we previously described.¹⁴ In brief, first we assessed the variation in the SNPs' effect sizes using 1,000 simulations when randomly excluding 266 cases and 173 controls (matching the numbers of overlapping samples). The variation in the IGAP effect sizes due to the overlap was estimated in terms of standard deviation ($SD_{IGAP} = 0.053$) from the mean (ie, the original IGAP SNP beta-coefficient [Beta_{IGAP}]). Then, new IGAP genome-wide summary statistics were simulated 10,000 times with adjusted effect sizes ($\text{Beta}_{adjusted}$) and p values for each SNP. $\text{Beta}_{adjusted}$ was sampled from a normal distribution with mean = Beta_{IGAP} and $SD = 0.053 * SE_{IGAP}$; p values_{adjusted} were

TABLE 2. ADNI Phenotypes and PET Amyloid Status

	Samples, n	n (% of MCI)	n (% of AD)	n (% of controls)
Amyloid positive	357	162 (47%)	120 (69%)	65 (29%)
Amyloid negative	304	148 (43%)	18 (10%)	128 (57%)
NA	89	34 (10%)	36 (21%)	31 (14%)
All samples	770	344	174	224

Shows number of individuals with positive/negative amyloid for clinically diagnosed samples (MCI, AD, and controls).

AD = Alzheimer disease; ADNI = Alzheimer's Disease Neuroimaging Initiative; MCI = mild cognitive impairment; NA = not available; PET = positron emission tomography.

redefined accordingly. At each simulation, SNPs were reselected and repruned based on LD $r^2 = 0.1$ and 1,000kb window. The prediction accuracies (areas under the receiver operator curve [AUCs]) reported in the Results section are presented as means from these 10,000 simulations.

Genome-wide and Pathway-Specific PRS Predictions

Initially, we tested whether PRSs are associated with AD risk (AD cases vs controls) in the ADNI dataset. Then we assessed whether the AD PRS can distinguish individuals with MCI from cognitively normal controls and amyloid-positive from amyloid-negative individuals. Finally, we assessed whether PRS can predict AD risk over and above *APOE* in MCI individuals who have had positive amyloid deposition (to be precise, the MCI individuals who converted to AD between the baseline and final time of assessment vs nonconverters). All analyses were performed using logistic regression models with the following predictors: (1) *APOE* ($\epsilon 2 + \epsilon 4$), (2) PRS without *APOE*, and (3) full PRS model (predictors 1 and 2 together). Gender and age were used as covariates in all analyses. We tested whether the PRS significantly improves the model fit over and above *APOE* alone with the *anova()* function in R. We report the accuracy of the models in terms of AUC. In addition, we calculated PRS prediction accuracies (AUCs) in the extremes of PRS distribution for individuals whose PRS score was greater or smaller than ± 1.5 SD from the PRS mean.

For the pathway-specific analyses, we chose the latest published 9 pathways that have been reported as playing a role in AD pathogenesis, namely (1) protein–lipid complex assembly, (2) regulation of beta-amyloid formation, (3) protein–lipid complex, (4) regulation of amyloid precursor protein catabolic process, (5) reverse cholesterol transport, (6) protein–lipid complex subunit organization, (7) plasma lipoprotein particle assembly, (8) tau protein binding, and (9) activation of immune response.⁶ Finally, to quantify the proportion of variance that remains unexplained by the pathways together, we calculated and tested PRS for the whole genome excluding these 9 pathways.

Pathway-specific PRSs were generated in the ADNI dataset for each individual as described above with and without the *APOE* region. The PRSs in this case were adjusted not only for 8 principal components but also for age and gender and then standardized.

The results were considered significant if the resulting p value was $\leq 1.85 \times 10^{-3} = 0.05/(3 \text{ scenarios} \times 9 \text{ pathways})$, corresponding to the Bonferroni correction for multiple comparisons.

Results

The prediction accuracy of AD cases ($n = 174$) versus controls ($n = 224$) at the last assessment point was $\text{AUC}_{\text{APOE}} = 76\%$ and $\text{AUC}_{\text{PRS}} = 75\%$, for *APOE* alone and for PRS without *APOE*, respectively (Table 3, first row). The best prediction accuracy ($\text{AUC}_{\text{FULL}} = 82\%$) was achieved with the full model, which includes both *APOE* and PRS. An analysis of variance test (last column of

Table 3) confirmed that PRS significantly improves the prediction accuracy of the model over and above *APOE* ($p = 1.7 \times 10^{-13}$). A similar pattern of results was observed when we compared MCI individuals at the last point of assessment ($n = 344$; see Table 1 for details) with controls; however, the accuracy was reduced ($\text{AUC}_{\text{APOE}} = 62\%$, $\text{AUC}_{\text{FULL}} = 68\%$). Again, PRS significantly improves the prediction accuracy of MCI risk over and above *APOE* ($p = 2.5 \times 10^{-11}$). Figure 1 shows standardized density plots of polygenic risk scores in AD cases (red line), controls (blue line), and MCI (orange line), where the mean of the PRS for the latter is between the means of the PRS for AD cases and controls. Interestingly, the results for prediction of amyloid deposition by PRS follows a different pattern; *APOE* alone significantly predicted amyloid deposition with $\text{AUC}_{\text{APOE}} = 76\%$, and PRS did not improve the prediction accuracy further.

When we tested the full PRS model for prediction of individuals at the extremes of polygenic score distribution (± 1.5 SD from the PRS mean), the prediction accuracy as expected increased (AUC = 94% for AD vs controls and AUC = 91% for MCI vs controls).

We tested whether the PRS can predict progression to AD in individuals with MCI. Of 459 individuals with MCI at the baseline assessment, 441 had known amyloid deposition status (270 were amyloid-positive and 171 were amyloid-negative). The prediction accuracy of amyloid deposition in this subsample was $\text{AUC}_{\text{APOE}} = 79\%$ by *APOE* alone and PRS did not improve the prediction accuracy ($p = 0.48$; Fig 2). Of 270 amyloid-positive individuals, 112 have progressed to AD and 150 individuals remained MCI as of the last point of assessment. In this case, PRS did predict AD progression ($\text{AUC}_{\text{APOE}} = 63\%$ and $\text{AUC}_{\text{FULL}} = 69\%$), significantly improving the prediction over and above *APOE* ($p = 0.0002$; see Fig 2).

Finally, we calculated pathway-specific PRSs and tested them for association with risk for AD, MCI, and amyloid deposition. The results are presented in Table 4. The majority of pathways were significantly associated with AD risk; however, this association was mostly driven by the *APOE* region. Two pathways (protein–lipid complex, protein–lipid complex subunit) remained significant after removing genes in the *APOE* region. When we excluded all pathways from the whole genome PRS, we observed that a substantial part of variance still remained unexplained ($p = 2.2 \times 10^{-14}$; last row of Table 4). Comparing amyloid-positive versus amyloid-negative individuals, the same 2 protein-lipid-related pathways and additionally reverse cholesterol transport were significant after removing genes in the *APOE* region. The association results of the 9 pathways' PRS with MCI risk were nominally significant for all pathways, and the association was mostly attributed

TABLE 3. PRS and APOE Predictions of AD/MCI/Controls/Amyloid Phenotypes in ADNI

Model	Statistical Characteristics	AD vs Controls, n = 174/224	MCI vs Controls, n = 344/224	Amyloid Positive vs Amyloid Negative, n = 357/304
<i>APOE</i>	Beta ^{1,3,4} [SE]	0.99 [0.13], -0.58 [0.22], 0.03 [0.01]	0.3 [0.1], -0.5 [0.17], -0.02 [0.01]	1.08 [0.01], 0.2 [0.17], 0.04 [0.01]
	p	1.06e-18	9.6e-5	<2.2e-16
	AUC ^a /AUC ^b	0.72/0.76	0.58/0.62	0.72/0.76
PRS (<i>p</i> < 0.5) without <i>APOE</i>	Beta ²⁻⁴ [SE]	0.93 [0.12], -0.7 [0.2], 0.016 [0.015]	0.68 [0.1], -0.47 [0.18], -0.007 [0.01]	0.3 [0.08], 0.13 [0.16], 0.023 [0.01]
	p	2.7e-18	6.e-12	1.4e-3
	AUC ^a /AUC ^b	0.74/0.75	0.66/0.67	0.58/0.58
Full PRS model	Beta ¹⁻⁴ [SE]	0.93 [0.13], 0.88 [0.13], -0.63 [0.24], 0.04 [0.02]	0.26 [0.1], 0.66 [0.1], -0.47 [0.18], -0.002 [0.01]	1.06 [0.1], 0.22 [0.09], 0.22 [0.17], 0.05 [0.01]
	p	1.9e-30	1.1e-12	2.3e-29
	AUC ^a /AUC ^b	0.81/0.82	0.67/0.68	0.75/0.76
ANOVA p (PRS above <i>APOE</i>)		1.7e-13	1.8e-10	0.038

Beta¹ = beta(e2 + e4), Beta² = beta(PRS), Beta³ = beta(sex), Beta⁴ = beta(age). First column shows 3 scenarios where PRS predictions were made: *APOE* alone, PRS without *APOE*, and full model (*APOE* plus PRS [*p* < 0.5]). Second column shows statistical characteristics that were calculated for each model; these include effect size (beta) with SE, *p* values, and AUC (with and without gender and age) and *p* value of significance of PRS above *APOE* model. Columns 3–5 represent 3 analyses with number of samples where different models were tested.

^aAUC without taking gender and age into account.

^bAUC where gender and age were used as predictors.

AD = Alzheimer disease; ADNI = Alzheimer's Disease Neuroimaging Initiative; ANOVA = analysis of variance; AUC = area under the curve; MCI = mild cognitive impairment; PRS = polygenic risk score; SE = standard error.

to *APOE*. This clearly demonstrates that the pathways that contain the *APOE* region are strong predictors of amyloid deposition. Protein–lipid complex has shown the strongest association with AD and amyloid deposition risk in all the

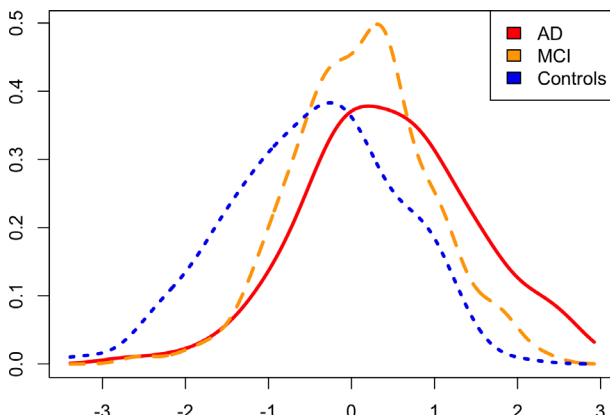


FIGURE 1: Density plots of polygenic risk score (PRS) for Alzheimer disease (AD), mild cognitive impairment (MCI), and cognitively normal participants. Standardized individual PRS scores for 3 phenotypes are shown (AD, MCI, and controls).

analyses. The overlap of genes in the 3 pathways above is presented in Figure 3.²⁷

Finally, we tested these pathways' PRS for association with amyloid deposition in individuals with MCI and with their further progression to AD when their amyloid deposition status was positive. We found that protein–lipid complex, protein–lipid complex subunit organization, and reverse cholesterol transport pathways are also associated with amyloid deposition even after exclusion of the *APOE* region (Table 5, 4th column).

Discussion

The pathological process related to AD starts long before clinical onset and lasts approximately 15 to 20 years.²⁸ It is widely believed that identifying individuals who have high risk of AD earlier is essential for therapeutic strategies for AD prevention and intervention.²⁹ Due to the diagnostic heterogeneity of MCI and different length of follow-up assessments, the conversion rate to AD or other types of

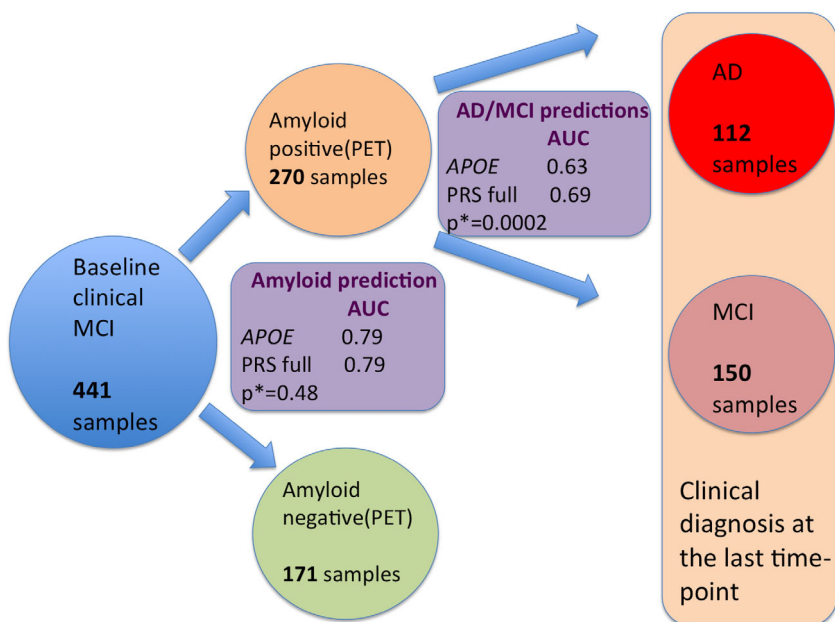


FIGURE 2: Diagram of prediction of amyloid deposition and further prediction of conversion of mild cognitive impairment (MCI) individuals to Alzheimer disease (AD) in the sample that was first clinically diagnosed with MCI using APOE and AD polygenic risk score (PRS). PRS predictions were first made for individuals who had baseline diagnosis of MCI. APOE alone and the full PRS model were used to predict amyloid deposition. The same models were used to predict which MCI individuals would convert to AD versus those individuals who had an MCI diagnosis using the latest clinical diagnosis. AUC = area under the curve; PET = positron emission tomography.

dementia varies widely over different studies.^{30,31} Identifying individuals with MCI and monitoring them through biomarker measurements should provide a better

understanding of the process of progression from MCI to AD. Although there is no generally accepted diagnostic criteria that specifies MCI individuals who will convert

TABLE 4. Prediction of AD and Amyloid Deposition Risk with Pathway-Specific PRSs

Pathways	Genes, n	AD (n = 174) vs Controls (n = 224)			Amyloid Positive (n = 357) vs Negative (n = 304)		
		Beta	p	p (no APOE region)	Beta	p	p (no APOE region)
Protein–lipid complex assembly	20	0.87	3e-13	0.35	0.94	4e-21	0.4
Regulation of beta-amyloid formation	10	0.79	1.1e-11	0.09	0.81	8.9e-17	0.47
Protein–lipid complex	40	0.91	8.14e-14	5.5e-3	0.96	1.8e-21	7.9e-3
Regulation of amyloid precursor protein catabolic process	12	0.79	1.1e-11	0.09	0.81	9.6e-17	0.49
Tau protein binding	11	0.77	3.1e-11	0.39	0.82	4.8e-17	0.6
Reverse cholesterol transport	17	0.84	2.4e-12	0.07	0.93	2.1e-19	0.03
Protein–lipid complex subunit organization	35	0.92	8.e-14	0.03	0.97	9.67e-22	0.03
Plasma lipoprotein particle assembly	18	0.89	2e-13	0.66	0.94	3.6e-21	0.98
Activation of immune response	432	0.18	0.06	0.06	0.21	6.8e-3	0.01
Whole genome without all pathways	–	0.93	2.2e-14	–	0.38	9.1e-6	–

First column shows names of pathways that were analyzed. Second column shows number of genes in each pathway. PRS pathway-specific effect sizes with p values and p values (no APOE region) of the models are presented in columns 3–8 for AD vs controls and amyloid deposition status. AD = Alzheimer disease; PRS = polygenic risk score.

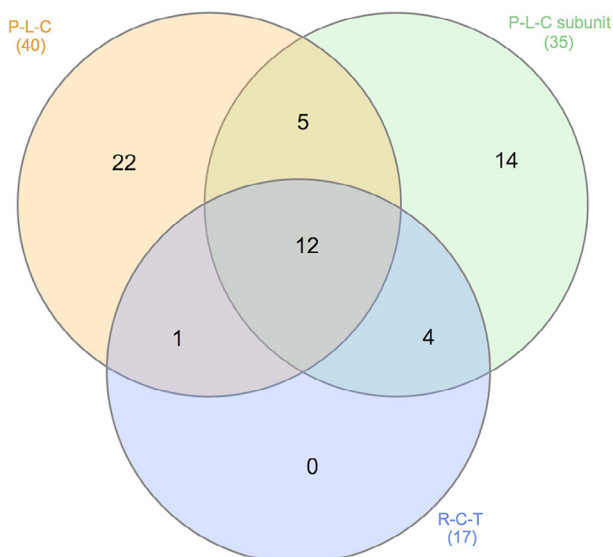


FIGURE 3: Overlap between 3 pathways: (1) protein-lipid complex (P-L-C; 40 genes), (2) protein-lipid complex subunit organization (35 genes), and (3) reverse cholesterol transport (R-C-T; 17 genes).

to AD, it is notable that an increase in amyloid plaques that starts many years before clinical symptoms appear plays an important role in brain degenerative changes.

A reasonable prediction accuracy can be achieved with a PRS approach that uses genetic profile information and relates it to AD risk.^{13,14} The PRS and its modifications have

been assessed for association with AD and AD-related phenotypes in a number of studies; however, the reported prediction accuracies have not been entirely consistent. In this study, we examined prediction accuracy that can be achieved with *APOE* alone and with the full PRS model differentiating between AD, MCI, controls, and amyloid status.

We have shown that the best prediction accuracy can be achieved with the PRS that includes *APOE* for both AD versus controls and MCI versus controls analyses (AUC = 82% and AUC = 68%, respectively). In both analyses, the PRS improves the prediction accuracy by about 8 to 9% compared to *APOE* alone, which replicates the analyses in independent datasets published elsewhere.^{13,14,16} Of course, GWASs indicate that *APOE* is the strongest risk factor and other common genetic variants have smaller effect sizes. However, the *APOE* region explains ~5% of SNP heritability, whereas the whole genome explains ~24%.³² In addition, PRS prediction accuracy shows a substantial increase in AUC, which makes the PRS potentially clinically useful for disease risk prediction. Furthermore, AD GWAS risk loci have greatly expanded our understanding of the disease mechanisms.

As expected, the accuracy of MCI prediction is lower than AD, which can be explained by the inclusion of a subset of MCI individuals who will not develop AD. For individuals with extreme PRS, the AUC reaches 90% and above for both AD and MCI.

TABLE 5. Prediction of Amyloid Deposition in Individuals with MCI and of Progression to AD in Individuals with MCI and Positive Amyloid Deposition with Pathway-Specific PRSs

Pathways	Amyloid Positive (n = 270) vs Amyloid Negative (n = 171)			MCI and Amyloid Positive (AD [n = 112] vs MCI [n = 150])		
	Beta	p	p (no <i>APOE</i> region)	Beta	p	p (no <i>APOE</i> region)
Protein–lipid complex assembly	1.11	1.92e-17	0.2	0.48	2.7e-4	0.81
Regulation of beta-amyloid formation	0.95	7.6e-14	0.2	0.30	9e-3	0.11
Protein–lipid complex	1.12	1.1e-17	3.1e-3	0.51	1.5e-4	0.23
Regulation of amyloid precursor protein catabolic process	0.95	8.4e-14	0.2	0.3	9.4e-3	0.12
Tau protein binding	0.99	2.2e-14	0.2	0.2	0.08	0.24
Reverse cholesterol transport	1.05	1.9e-15	0.03	0.31	0.01	0.24
Protein–lipid complex subunit organization	1.1	1.2e-17	0.05	0.51	1.9e-4	0.64
Plasma lipoprotein particle assembly	1.09	3.4e-17	0.9	0.51	1e-4	0.31
Activation of immune response	0.18	0.068	0.09	0.08	0.54	0.76
Whole genome PRS without pathways	0.36	2.1e-3	–	0.6	8.8e-5	–

First column shows names of pathways that were analyzed. PRS pathway-specific effect sizes with p values and p values (no *APOE* region) of the models are presented in columns 2–7.

AD = Alzheimer disease; MCI = mild cognitive impairment; PRS = polygenic risk score.

The prediction of amyloid deposition showed a different pattern. In the whole sample, the prediction accuracy with *APOE* alone was 76% and the PRS did not improve the accuracy any further (AUC remained 76%). Similar results were obtained when we tested the prediction accuracy of amyloid deposition in individuals with MCI. However, when we looked at individuals who have already had positive amyloid deposition and attempted to predict their progression to AD, the best accuracy was observed with the full PRS model, which includes the *APOE* region; however, this also requires the PRS component.

Note that for all the models used, the best prediction accuracy was achieved with a *p* value threshold of 0.5 for AD-associated SNPs. The same threshold was previously reported in studies that were done on different genotyping arrays.^{13,14} For the best prediction accuracy in clinical practice, PRS should be generated on a set of SNPs in a way that captures genetic liability of the whole genome.

The potential implication of these findings is that the *APOE* gene affects amyloid deposition but that much of the rest of the risk of disease is involved in the rate at which amyloid deposition causes a neurodegenerative response. Clinical trials have previously shown that there is little correlation between AD progression and accumulation of amyloid plaques, supporting a hypothesis that AD development may have 2 separated stages: amyloid dependent and amyloid independent.³³ It is also known that the *APOE* gene influences the deposition of amyloid in the brain³⁴ and that this is necessary but not sufficient for development of clinical AD. Moreover, it has been shown that neuronal loss and tangle numbers increase as AD progresses,³⁵ unlike the number of amyloid plaques, which reaches its maximum³⁶ with the onset of clinical symptoms.

While analysis of early onset AD firmly implicated amyloid precursor protein metabolism and Aβ production in the etiology of the disease, GWASs and exome and genome sequencing have implicated with varying degrees of confidence a number of potentially biologically relevant pathways in late onset AD pathogenesis.^{21,22} Of course, pathway construction is an imperfect art both because of the knowledge base used in the generation of the pathways and because proteins may have more than one function in more than one cell type. Nevertheless, it is valuable to divide polygenic risk by pathways both in terms of modeling the disease through induced pluripotent stem cell technologies (one might like to assign high or low risk by pathway) and in terms of eventually tailoring therapies to pathway deficits. To dissect AD PRS by biologically relevant gene sets, we tested pathways enriched in AD⁶ identified by IGAP. All pathways except “activation of immune response” were highly significantly associated with AD risk and amyloid deposition risk; however, most of the signal was attributed to the *APOE* region

alone. Protein–lipid complex showed the strongest association with AD and amyloid deposition risk in all the analyses.

In conclusion, our results imply that *APOE* contributes to disease risk in a manner that is mechanistically different from the other genetic contributors to disease risk. We speculate that *APOE* affects amyloid deposition and that the PRS affects conversion from amyloid positivity to AD. Therefore, in the context of the amyloid cascade hypothesis, *APOE* acts prior to amyloid deposition and the remaining genetic risk factors identified through GWASs act between amyloid deposition and clinical onset of AD.

Acknowledgment

This study was supported to J.H. by the Dolby Foundation and an anonymous donor. Collection and sharing for this project were funded by ADNI (National Institutes of Health grant U01 AG024904) and Department of Defense (DOD) ADNI (DOD award number W81XWH-12-2-0012).

ADNI is funded by the National Institute of Aging, the National Institute of Biomedical Imaging and Bioengineering, and through generous contributions from the following: AbbVie, Alzheimer’s Association, Alzheimer’s Drug Discovery Foundation, Araclon Biotech, BioClinica, Biogen, Bristol-Myers Squibb, CereSpin, Cogstate, Eisai, Elan Pharmaceuticals, Eli Lilly and Company, EuroImmun, F. Hoffmann-La Roche and its affiliated company Genentech, Fujirebio, GE Healthcare, IXICO, Janssen Alzheimer’s Immunotherapy Research and Development, Johnson & Johnson Pharmaceutical Research & Development, Lumosity, Lundbeck, Merck & Co, Meso Scale Diagnostics, NeuroRx Research, Neurotrack Technologies, Novartis Pharmaceuticals Corporation, Pfizer, Piramal Imaging, Servier, Takeda Pharmaceutical Company, and Transition Therapeutics. The Canadian Institutes of Health Research provides funds to support ADNI clinical sites in Canada. Private sector contributions are facilitated by the Foundation for the National Institutes of Health (<https://fnih.org/>). The grantee organization is the Northern California Institute for Research and Education, and the study is coordinated by the Alzheimer’s Therapeutic Research Institute at the University of Southern California. ADNI data are disseminated by the Laboratory for Neuro Imaging at the University of Southern California.

We thank the MRC Centre for Neuropsychiatric Genetics and Genomics, the UK Dementia Research Institute, Dementia Platform UK, and InnovateUK; IGAP for providing summary results data for these analyses; and the ADNI database. The investigators within IGAP contributed to the design and implementation of IGAP and/or provided data but did not participate in the analysis or writing of this report.

Author Contributions

G.L., M.S., E.B., and R.S. contributed to the acquisition and data analysis; G.L., M.S., E.B., R.S., J.H., and V.E.-P. contributed to the drafting of the manuscript or part of it; J.H., J.W., and V.E.-P. contributed to the critical review of the manuscript; J.H., J.W., and V.E.-P. contributed to the conception and design of the study.

Potential Conflicts of Interest

Nothing to report.

References

1. Sloane PD, Zimmerman S, Suchindran C, et al. The public health impact of Alzheimer's disease, 2000–2050: potential implication of treatment advances. *Annu Rev Public Health* 2002;23:213–231.
2. Lambert JC, Ibrahim-Verbaas CA, Harold D, et al. Meta-analysis of 74,046 individuals identifies 11 new susceptibility loci for Alzheimer's disease. *Nat Genet* 2013;45:1452–1458.
3. Jones L, Lambert J-C, Wang L-S, et al. Convergent genetic and expression data implicate immunity in Alzheimer's disease. *Alzheimers Dement* 2014;11:658–671.
4. Escott-Price V, Bellenguez C, Wang LS, et al. Gene-wide analysis detects two new susceptibility genes for Alzheimer's disease. *PLoS One* 2014;9:e94661.
5. Sims R, Van Der Lee SJ, Naj AC, et al. Rare coding variants in PLCG2, ABI3, and TREM2 implicate microglial-mediated innate immunity in Alzheimer's disease. *Nat Genet* 2017;49:1373–1384.
6. Kunkle BW, Grenier-Boley B, Sims R, et al. Meta-analysis of genetic association with diagnosed Alzheimer's disease identifies novel risk loci and implicates Abeta, Tau, immunity and lipid processing. *Nat Genet* 2019; 51:414–443. <https://www.biorxiv.org/content/early/2018/04/05/294629.full.pdf+html>
7. Corder EH, Saunders AM, Strittmatter WJ, et al. Gene dose of apolipoprotein E type 4 allele and the risk of Alzheimer's disease in late onset families. *Science* 1993;261:921–923.
8. Vos SJB, Verhey F, Frölich L, et al. Prevalence and prognosis of Alzheimer's disease at the mild cognitive impairment stage. *Brain* 2015;138:1327–1338.
9. Erratum: Predictive accuracy of amyloid imaging for progression from mild cognitive impairment to Alzheimer disease with different lengths of follow-up: a systematic review. *Medicine (Baltimore)* 2015;94:1.
10. Petersen RC, Negash S. Mild cognitive impairment: an overview. *CNS Spectr* 2008;13:45–53.
11. McKhann GM, Knopman DS, Chertkow H, et al. The diagnosis of dementia due to Alzheimer's disease: recommendations from the National Institute on Aging-Alzheimer's Association workgroups on diagnostic guidelines for Alzheimer's disease. *Alzheimers Dement* 2011;7:263–269.
12. Albert MS, DeKosky ST, Dickson D, et al. The diagnosis of mild cognitive impairment due to Alzheimer's disease: recommendations from the National Institute on Aging-Alzheimer's Association workgroups on diagnostic guidelines for Alzheimer's disease. *Alzheimers Dement* 2011;7:270–279.
13. Escott-Price V, Sims R, Bannister C, et al. Common polygenic variation enhances risk prediction for Alzheimer's disease. *Brain* 2015; 138:3673–3684.
14. Escott-Price V, Myers AJ, Huentelman M, Hardy J. Polygenic risk score analysis of pathologically confirmed Alzheimer disease. *Ann Neurol* 2017;82:311–314.
15. Adams HHH, de Brujin RFAG, Hofman A, et al. Genetic risk of neurodegenerative diseases is associated with mild cognitive impairment and conversion to dementia. *Alzheimers Dement* 2015;11:1277–1285.
16. Logue MW, Panizzon MS, Elman JA, et al. Use of an Alzheimer's disease polygenic risk score to identify mild cognitive impairment in adults in their 50s. *Mol Psychiatry* 2019;24:421–430.
17. Darst BF, Kosik RL, Racine AM, et al. Pathway-specific polygenic risk scores as predictors of amyloid- β deposition and cognitive function in a sample at increased risk for Alzheimer's disease. *J Alzheimers Dis* 2017;55:473–484.
18. Leonenko G, Sims R, Shoai M, et al. Polygenic Risk and Hazard Scores for Alzheimer's disease prediction. *Ann Clin Transl Neurol* 2019;6:456–465.
19. Tan CH, Fan CC, Mormino EC, et al. Polygenic hazard score: an enrichment marker for Alzheimer's associated amyloid and tau deposition. *Acta Neuropathol* 2018;135:85–93.
20. Tan CH, Bonham LW, Fan CC, et al. Polygenic hazard score, amyloid deposition and Alzheimer's neurodegeneration. *Brain* 2019;142:460–470.
21. Jones L, Holmans PA, Hamshere ML, et al. Genetic evidence implicates the immune system and cholesterol metabolism in the aetiology of Alzheimer's disease. *PLoS One* 2010;5:e13950.
22. Hardy J, Bogdanovic N, Winblad B, et al. Pathways to Alzheimer's disease. *J Intern Med* 2014;275:296–303.
23. Mueller SG, Weiner MW, Thal LJ, et al. Ways toward an early diagnosis in Alzheimer's disease: the Alzheimer's Disease Neuroimaging Initiative (ADNI). *Alzheimers Dement* 2005;1:55–66.
24. Petersen RC, Aisen PS, Beckett LA, et al. Alzheimer's Disease Neuroimaging Initiative (ADNI): clinical characterization. *Neurology* 2010; 74:201–209.
25. Anderson CA, Pettersson FH, Clarke GM, et al. Data quality control in genetic case-control association studies. *Nat Protoc* 2010;5:1564–1573.
26. Purcell SM, Wray NR, Stone JL, et al. Common polygenic variation contributes to risk of schizophrenia and bipolar disorder. *Nature* 2009;460:748–752.
27. Heberle H, Meirelles VG, da Silva FR, et al. InteractiVenn: A web-based tool for the analysis of sets through Venn diagrams. *BMC Bioinformatics* 2015; 16(1): 169.
28. Jack CR, Holtzman DM. Biomarker modeling of Alzheimer's disease. *Neuron* 2013;80:1347–1358.
29. Karra E, Hardy J. A critique of the drug discovery and phase 3 clinical programs targeting the amyloid hypothesis for Alzheimer disease. *Ann Neurol* 2014;76:185–205.
30. Ganguli M, Snitz BE, Saxton JA, et al. Outcomes of mild cognitive impairment by definition: a population study. *Arch Neurol* 2011;68: 761–767.
31. Gabryelewicz T, Styczynska M, Luczywek E, et al. The rate of conversion of mild cognitive impairment to dementia: predictive role of depression. *Int J Geriatr Psychiatry* 2007;22:563–567.
32. Escott-Price V, Shoai M, Pither R, et al. Polygenic score prediction captures nearly all common genetic risk for Alzheimer's disease. *Neurobiol Aging* 2017;49:214.e7–214.e11.
33. Hyman BT. Amyloid-dependent and amyloid-independent stages of Alzheimer disease. *Arch Neurol* 2011;68:1062–1064.
34. Musiek ES, Holtzman DM. Three dimensions of the amyloid hypothesis: time, space and "wingmen." *Nat Neurosci* 2015;18:800–806.
35. Ingelsson M, Fukumoto H, Newell KL, et al. Early A β accumulation and progressive synaptic loss, gliosis, and tangle formation in AD brain. *Neurology* 2004;62:925–931.
36. Hyman BT, Marzollo K, Arriagada PV. The lack of accumulation of senile plaques or amyloid burden in Alzheimer's disease suggests a dynamic balance between amyloid deposition and resolution. *J Neuropathol Exp Neurol* 1993;52:594–600.